



A machinability evaluation based on the thermal and mechanical properties of two engine valve steels

Marta Regina Delle Donne Carvalho¹ · Armando Ítalo Sette Antonialli² · Anselmo Eduardo Diniz¹

Received: 19 June 2020 / Accepted: 15 September 2020 / Published online: 21 September 2020
© Springer-Verlag London Ltd., part of Springer Nature 2020

Abstract

Iron-based superalloys are difficult to machine because of their thermal and mechanical properties provided by alloying elements as nickel, chromium, titanium, and aluminum. However, parts made with this kind of material has to be machined during their production processes. In this work, two different automotive engine valve steel grades, VAT 30® and VAT 36®, were compared in terms of machinability, considering cutting power consumption, roughness of the machined surface, and tool life, besides the identification of the main tool wear mechanisms that have led to the end of tool life. The main goal of this work is to understand the difference in these machining outputs based on the thermal and mechanical properties of these two materials. In order to reach this goal, turning tests were held using two different cooling conditions, conventional and high-pressure coolant. Also, two PVD-coated carbide inserts were applied, one with negative rake angle and another neutral. Finally, cutting speed was tested in two levels, providing a full 2⁴ factorial planning. Results show that VAT 30® has shown higher machinability in terms of tool life in almost every condition, although this steel presents higher hardness, mechanical strength, and strain hardening coefficient, besides lower thermal conductivity. However, it also presents lower ductility and abrasiveness, features that retarded abrasion and attrition as tool wear mechanisms, in such a way that tool life could have been lengthened.

Keywords Turning · Cutting speed · Cutting tool geometry · High-pressure coolant

1 Introduction

Alloy design and improvements of austenitic steels for exhaust valve applications have taken place since the 1980s. Steel alloys 23-8N and modified 21-4N are still used today in some applications, although their mechanical properties are clearly inferior to alloys with intermediate Ni content and Ni-based superalloys, in part due to the significantly lower cost of the previous compared to the last. Because of that, recent developments of intermediate Ni-based alloys, which contain lower amounts of costly Ni, utilize novel alloy design strategies to provide similar or greater mechanical properties than some Ni-based superalloys [1].

UNS N07751 and UNS N07080 alloys, for example, present high hot hardness and resistance to oxidation, corrosion, and creep, but also present low wear resistance and high cost due to the high nickel contents. New Ni-based alloys for application in high-performance automotive valves, like VAT 32® and VAT 36®, are based on a high nickel-chromium austenitic matrix with the dispersion of second phases like Ni₃(Al,Ti,Nb), Ni₃Nb, and NbC, presenting an economical advantage for substitution of the former alloys, besides higher resistance to abrasive wear and higher fatigue strength [2].

According to Silva and Mei [3], the addition of nickel into alloy steels increases both mechanical strength and toughness, due to solid solution. Besides that, nickel also stabilizes austenite, even when high chromium contents are present. Chromium addition provides higher resistance to corrosion and oxidation, while titanium provides hardening due to precipitation. Aluminum addition may avoid grain coarsening and improve wear resistance, while niobium can provide resistance in high temperatures.

The addition of great amounts of some alloying elements may insert those alloys into an as-called superalloys group. These materials exhibit high heat resistance and melting points,

✉ Armando Ítalo Sette Antonialli
antonialli@ufscar.br

¹ Faculty of Mechanical Engineering, University of Campinas, Campinas, Brazil

² Center for Exact Sciences and Technology, Federal University of São Carlos, São Carlos, Brazil

features that make them good candidates for the manufacture of aero-engine components for example. These exotic superalloys can be grouped into four major categories: nickel-based, cobalt-based, iron-based, and titanium alloys. The main use of iron-based superalloys that are weaker at elevated temperatures than nickel alloys is in chemical processing applications such as heat exchanger, piping, retorts, mixing tanks, heat treatment equipment, muffles, conveyors, baskets, and boxes [4].

The term machinability is not unambiguous, although it may be taken to imply that it can be clearly defined and quantified. Anyway, how easy a machining operation can be may be assessed by criteria such as tool life, cutting forces, surface finish, and chip morphology. Machinability ratings for any given material can be experimentally determined setting cutting tool and cutting conditions [5]. Regarding this, Yamane et al. [6] proposed criteria they called difficult-to-cut rating (DTCR), which is expressed by the area of a radar chart that considers hardness, mechanical strength, elongation, and thermal attributes of the material being cut. These features maintain a close relationship with tool life, cutting forces, and surface finishing. The smaller the chart area, the better the material machinability.

Superalloys present lower machinability than austenitic stainless steels. Their abrasive phases lead to adhesive and abrasive wear of the cutting tool and to the risk of plastic deformation. The addition of nickel or cobalt in these alloys may increase the risk of adhesion of the workpiece material on the cutting tool. The addition of elements that form oxides and/or carbides, such as chromium, vanadium, tungsten, or aluminum, may cause abrasive tool wear. Titanium addition may reduce thermal conductivity and, therefore, increase the temperature of the cutting edge, accelerating tool wear. A high manganese content on austenitic steels or duplex stainless steels makes them particularly susceptible to strain hardening, which means an increase in the number of dislocations and resistance to further deformations [7].

Asha et al. [8] have compared the machinability of two alloy steel grade EN24 and high carbon high chromium (HCHCr) in terms of tool life in turning with multilayer-coated carbide inserts. HCHCr grade steel presents higher carbon, silicon, manganese, chromium, molybdenum, and lower nickel content than AN24 grade, besides higher hardness (286 HB against 210 HB). Their results have shown that HCHCr grade provides shorter tool life than EN24 grade, as expected, because of the high alloying elements and higher hardness presented. They also concluded that flank wear and crater wear were always determinant to the end of tool life when machining EN24 steel grade, while, for HCHCr steel grade, these mechanisms were observed only for lower cutting conditions, since plastic deformation was verified at higher machining parameters.

Vinoth Jebaraj et al. [9] claim that the machinability of duplex stainless steel DSS 2205 is poor when compared to

conventional austenitic grades such as 316L and 304L especially because of the higher thrust force that is required due to its high-temperature tensile strength. It is important to remember that, because surface finish and topography play a major role in determining the life span of DSS in marine exposure, sometimes either polishing, shot peening or other finishing processes may be needed. For super duplex DSS 2507, machinability is even worse.

Denkena et al. [10] observed the formation of serrated chips during the turning of aluminum-alloyed ultra-high-carbon steels (UHC), a feature that imposes a limit on the productivity of this manufacturing process. These materials are composed of a soft ferrite-like matrix with embedded carbides, and it has been shown that the different hardness of the second-phase particles can be explained due to an altered bonding. They have shown that dispersions along the grain boundaries containing manganese, phosphorus, and carbon are expected to reduce the intergranular cohesion, resulting in a brittle material behavior despite a soft matrix. On the other side, the use of tools with negative rake angles leads to serrated chip formation due to instabilities in the primary shear zone, which may arise from microcracks that connect voids along the grain boundaries. Then, neutral or positive rake angles should be selected in order to avoid intense dynamic loads on the tool. Besides that, coated carbide tool should be chosen to prevent the observed diffusion processes between WC-Co from the cemented carbide tool and the matrix of the UHC steel. The use of cooling is also recommended.

Rocha et al. [11] have investigated the influence of cutting speed, depth of cut, and feed rate on the machining of valve seats of internal combustion engines made of a Fe-C-Cu-Ni-Mo alloy obtained from powder metallurgy using polycrystalline cubic boron nitride (PCBN) tools. Besides the expected harmful influence of feed on surface roughness, they concluded that the main tool wear mechanisms were attrition at low cutting speeds, diffusion at medium speeds and, at high speeds, the tool had undergone microchipping.

Liu et al. [12] have investigated the effect of face milling parameters on the surface properties and fatigue strength of Incoloy A286, an iron-base superalloy widely used in gas turbine jet engines and other similar applications. Their results have showed that there are optimum values for cutting speed and feed rate in terms of work hardening, grain refinement, surface yield strength, and tensile residual stresses. Because of the severe stress relaxation, it was not possible to infer the effect of residual stresses on the fatigue life under different cutting parameters.

Tian et al. [13] have studied the performance of a graded ceramic tool in high-speed turning of the age-strengthened-type iron-based superalloy GH2132. They have concluded that cutting speed could change the form of the chips, which were closely related to tool wear. Cutting temperature and cutting forces have been reduced by the employment of the

graded ceramic tool due to the alleviation of thermal-mechanical stresses. Consequently, tool life has shown to be longer, although grooving, at low speeds, and notching of the tool, at high speeds, had been reported. Surface roughness results were better for high cutting speeds.

Davoodi and Eskandari [14] have investigated the optimization of tool life and volume of material removed besides tool wear mechanisms present when turning N-155 iron-nickel-base superalloy with cemented carbide inserts. Using the analysis of variance (ANOVA) and response surface methodology (RSM), they have concluded that the optimum cutting variables for a maximum volume of material removed in minimum cutting time were cutting speed of 85.55 m/min and feed rate of 0.2 mm. Analysis of tool wear mechanisms showed that the most dominant tool failure modes were adhesion wear.

According to Stahl et al. [7], the following features severely impair the machinability of steels: hardness, ultimate tensile strength, thermal conductivity, abrasiveness, strain hardening exponent, ductility, and specific heat. Although a small increase of hardness may avoid the built-up edge formation when machining low carbon alloys, further increase of hardness may speed up tool wear due to abrasion and diffusion. Shearing is closely related to tensile strength, so that increasing this property may rise cutting temperature and, consequently, impair machinability. Of course, thermal conductivity affects machinability positively as it reduces cutting temperature and so tool wear rate is diminished. Regarding the machinability of multi-phase steels, it is common that the most fragile phase is also the hardest one. Abrasiveness is usually related to the difference of hardness between matrix and precipitates, besides their sizes and distribution. Low carbon steels are commonly more adhesive, while high carbon steels tend to be more abrasive. High strain hardening exponent considerably affects chip formation, reducing the machinability of steels especially when low thermal conductivity is also present. High ductility affects the minimum radius for chip breakability; with low ductility, small chips are produced and machinability is increased because friction is reduced as well as the tendency for built-up edge formation. Finally, specific heat is the most important variable over cutting temperature as its increase decreases the cutting temperature and so provides longer tool lives and, therefore, higher machinability.

It is important to highlight that, besides the thermal and mechanical properties of the material that is being cut, cutting parameters, cooling-lubrication conditions, tool sharpness, tool grade, and geometry (especially the rake angle) severely impair specific cutting pressure and, therefore, cutting power. As an example, cutting force may face a 25% increase from the beginning to the end of tool life. Very negative tool rake angles may impair cutting force significantly; negative five degrees mean close to a 10% increase in cutting force [15].

Regarding the surface roughness, it should be remembered that, along the tool path over the workpiece, there is

a region, very close to the material that becomes chip, which undergoes plastic deformation although it will not be separated from the part that is being machined. This plastic formation becomes burrs, imposing severe difficulties to obtain smooth finishing, especially when very ductile materials are being cut [16].

Before finishing this review of literature, it is important to describe some of the main tool wear mechanisms, since an alloy machinability depends on how the thermal and mechanical properties of the material influence the way it causes tool wear. One of the main tool wear mechanisms is mechanical abrasion, i.e., the tool friction against either the hard particles of a rigid element such as the workpiece or a flexible element such as the chip. This mechanism is frequently responsible for the formation of flank wear in high cutting speeds [17].

An incentive for the appearance of abrasion on the tool, which is identified by the presence of abrasive scratches parallel to the material flow on the tool flank face, is the cutting temperature increase, which reduces the tool hardness and, consequently, its abrasion resistance. The abrasion mechanism causes the tool coating removal, what increases the tool friction coefficient and, consequently, makes possible the appearance of another tool wear mechanism, called by Trent and Wright [18] as attrition, which gives a rough aspect to the worn region. In this mechanism, the chip being formed adheres to the tool but, cyclically, this adhered layer is removed by the relative movement between the elements in contact. This removal does not occur in the interface of the two surfaces but causes the removal of particles from the tool. This tool particles, very hard, goes its way on the interface causing further friction with the tool, removing even more tool material by abrasion. Besides depending on cutting temperature, attrition depends also on the workpiece material ductility. The more ductile, the higher its tendency to adhere. This mechanism is responsible for both crater wear and flank wear. For the occurrence of attrition on the tool flank face to cause flank wear, it is necessary that part of the chip being formed be extruded between tool and workpiece and, therefore, adheres to the flank face. For this to occur, some vibration between tool and workpiece must happen, in order to generate some space between these two elements and, therefore, to make extrusion possible [17, 18].

In this work, the machinability of two different iron-based superalloys (VAT 30® and VAT 36®) for engine valves manufacturing, considering cutting parameters for finishing operations, is compared in terms of cutting power consumption, arithmetical mean roughness value, tool life, and tool wear mechanisms. Input variables that were studied include also cutting speed, cooling condition, and tool geometry. The main objective is to understand the relation between the alloy mechanical and thermal properties with these output variables of the turning process.

2 Materials and Methods

The turning tests were performed in a CNC Lathe, with 15 kW main power and 4500 rpm maximum revolutions. External straight turning tests were carried out on two different valve steel grades—VAT 30® and VAT 36®—which were provided as 4 ½ in. diameter and 200-mm length shafts. Chemical composition (in weight percent, wt%) and physical and mechanical properties of these steels may be seen in Tables 1, 2, and 3 respectively. Both of them are recommended for valve manufacture for internal combustion engines, in which high-temperature strength and corrosion resistance are necessary. As already cited in this work, nickel is a very expensive alloying element. So VAT 30® alloy is an attempt to replace VAT 36® alloy, which is more expensive due to its higher Ni content. Therefore, it is reasonable to compare the machinability of such similar materials which present different nickel content.

As it will be understood ahead, some additional characterization of both superalloys was necessary to explain the results of the machining experiments. For that, a scanning electron microscope (SEM) Zeiss EVO MA15 with an energy-dispersive x-ray spectroscopy (EDS) resource was used to evaluate the abrasiveness of VAT 30® and VAT 36®. Figure 1 presents an overview of VAT 30® (Fig. 1a) and VAT 36® (Fig. 1b) after sanding, polishing, and etching. It can be clearly seen the carbide inclusions (dark regions) on the matrix (white background) of both superalloys. The identification of these two phases was confirmed by chemical microanalysis, as it will be explained ahead. Using ImageJ, a free-ware software on image processing, it was easy to infer that VAT 36® presents a higher percentage of an area full of

Table 1 Chemical composition of VAT 30® and VAT 36® valve steel grades [19]

Chemical element	VAT 30® (wt%)	VAT 36® (wt%)
Fe	Balance	Balance
Ni	30.00–33.00	~ 36.00
Cr	13.5–15.5	~ 19.00
Ti	2.40–2.90	~ 1.20
Al	1.70–2.10	~ 1.95
Co	1.00 max	–
Mo	0.60–0.80	–
Nb	0.55–0.80	~ 2.00
Si	0.50 max	–
Mn	0.50 max	0.50 max
Cu	0.50 max	–
W	0.50 max	–
C	0.03–0.08	0.04–0.06
P	0.015 max	–
S	0.010 max	0.50 max

Table 2 Physical properties of VAT 30® and VAT 36® valve steel grades [19]

Property	VAT 30®	VAT 36®
Specific mass (kg/m ³ , 25 °C)	7861.1	7870.9
Specific heat capacity (J/kg K, 750 °C)	823.5	810.4
Thermal conductivity (W/m K, 700 °C)	17.4	24.2

carbides; nonetheless, the average size of them is reasonably higher than the average size of carbides in VAT 30®.

Finally, the EDS feature was capable of identifying the main carbides present in each of the SEM analysis shown in Fig. 2. The carbides present in VAT 30® (points 1, 2, 3, and 4 in Fig. 2a) are rich in Nb and Ti, as inclusions on the austenitic matrix with Fe, Ni, and Cr (points 5 and 6). Similarly, the carbides present in VAT 36® (points 1, 2, and 3 in Fig. 2b) are also rich on Nb and Ti, as inclusions on the austenitic matrix with Fe, Ni, and Cr (points 4 and 5), but the presence of Nb was heavier than on VAT30 carbides.

Considering that NbC (which presents higher content in VAT 36®) is considerably harder than TiC, the amount of carbides in VAT36® is higher than in VAT30® and, besides that, those inclusions measured in VAT 36® are quite smaller, and therefore, are likely to be more coherent to the matrix (that is, more difficult to remove); it can be inferred that VAT 36® presents higher abrasiveness than VAT 30®.

During the machining tests, cutting power consumption was monitored using an Embrasul RE 4001 energy analyzer connected to a portable computer. The three electrical phases of the CNC lathe motor were used to acquire both electric tension and current. The results that will be shown represent only the active power (the one which performs the work) regarding each machining test, subtracting the offset (related to the energy that is necessary to keep the machine working and the spindle on) from the global power measured. Between one and another machining pass, the arithmetical mean roughness value (R_a) of the machined surface of the workpiece was evaluated using Mitutoyo SurfTest SJ-201P portable surface roughness tester adjusted for a 0.8-mm cutoff. The evolution of the maximum flank wear (V_{BBmax}) of the tools was systematically measured using an Olympus MX51-M optical

Table 3 Mechanical properties of VAT 30® and VAT 36® valve steel grades [19]

Property	VAT 30®	VAT 36®
Hardness (HV, 760 °C)	299	270
Ultimate tensile strength (MPa, room)	1087.6	1017.1
Elongation (% , room)	28.1	31.3
Strain hardening exponent	1.4×10^{-3}	1.0×10^{-3}

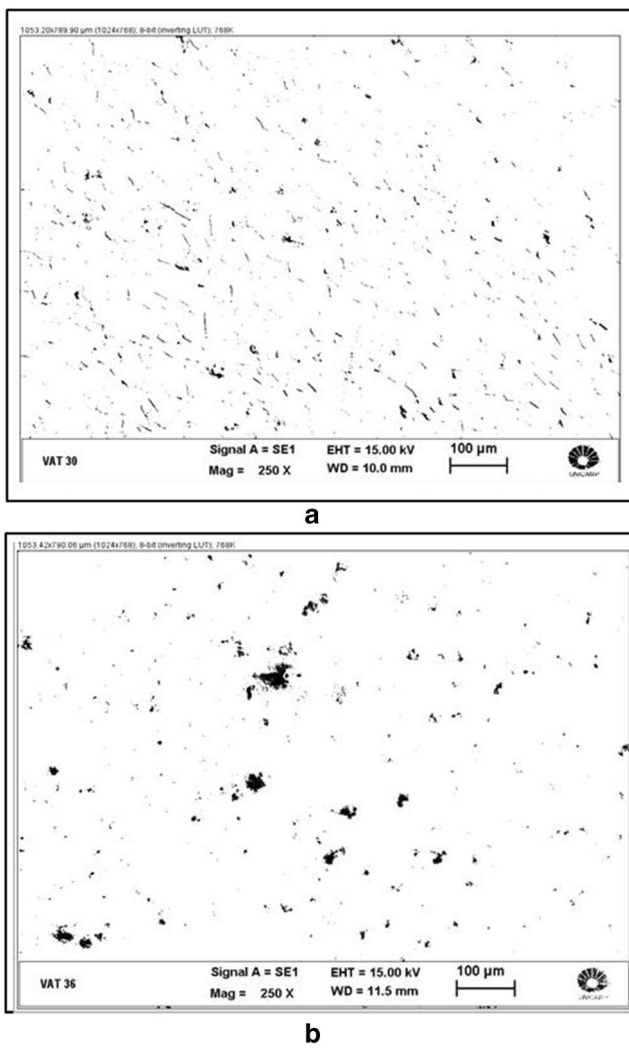


Fig. 1 SEM on a VAT 30® and b VAT 36®

microscope with a 1.3 megapixels Motic Moticam 1000 optical camera connected to a portable computer along with the image processing software Motic Images Plus. An experiment was considered finished when the tool wear had reached 0.3 mm, the tool life criterion applied here. After all machining tests, SEM with EDS resource Zeiss EVO MA15 was also used to investigate the wear mechanisms which led to the end of each tool life.

Tool life was measured in terms of volume of material removed during each (V, cm^3). It may be calculated as tool life measured in time (T, min) times material removal rate ($\text{MRR}, \text{cm}^3/\text{min}$), which means T times cutting speed ($v_c, \text{m/min}$), times feed (f, mm), times depth of cut (a_p, mm), as it follows in Eq. 1.

$$V = T \cdot \text{MRR} = T \cdot v_c \cdot f \cdot a_p \quad (1)$$

The experimental planning chosen for this work was a full 2^4 factorial, which means that four input variables were

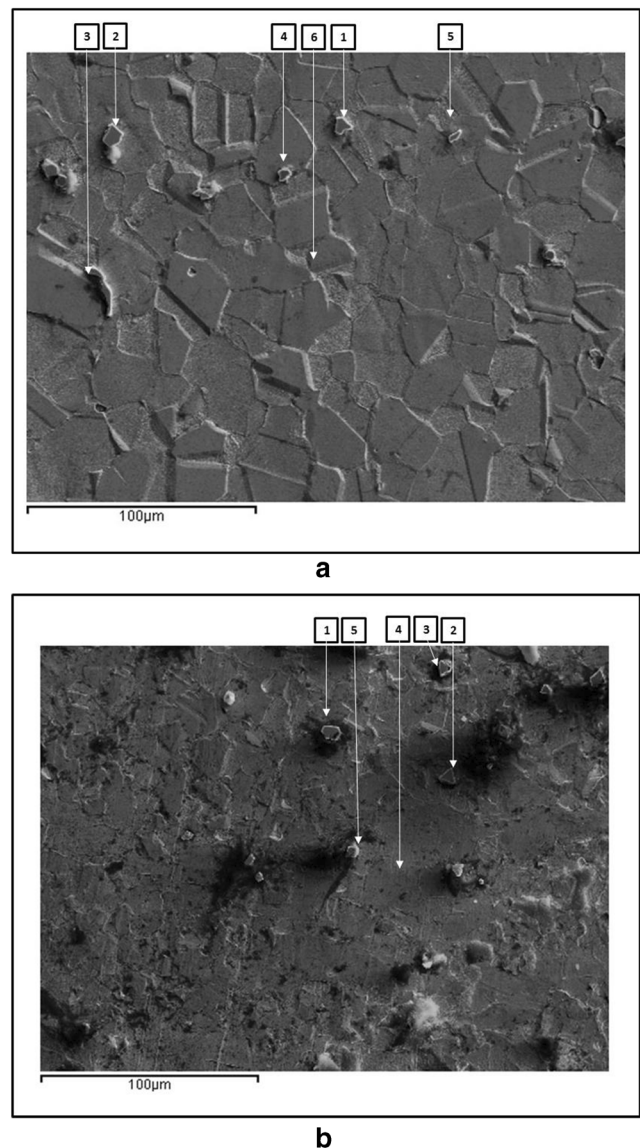


Fig. 2 EDS on a VAT 30® and b VAT 36® carbides

studied, each one applied at two different levels. The first variable is, of course, the valve steel grade for the workpiece material, as it has already been stated, VAT 30® and VAT 36®. The second input variable was the cooling condition, also tested on two levels: conventional coolant and high-pressure coolant (approximately 70 bar injected towards the tool rake face); in both cases, a Blaser Swisslube vegetal-based emulsion (6% Brix) was employed. The third input variable was tool geometry. Two different tools were tested; one was a negative rake angle ($\gamma_o = -6^\circ$) PCLNR 2525 M12 HP with CNMG 120404 MF PVD triple-layered (TiAlN/(Al,Cr)2O3/TiAlN)-coated carbide inserts, ISO grade HC M15; the other one was a neutral rake angle ($\gamma_o = 0^\circ$) SCLCR 2525 M09 HP with CCMT 09T304 MF PVD-coated carbide inserts of the same grade. Both of them presented a nose radius of 0.4 mm and a cutting edge angle of

95°. Finally, for the fourth variable, cutting speed (v_c) was tested at two levels: one value according to the toolmaker recommendations, 70 m/min, and a value of 20% higher, then 85 m/min. Results were compared considering a 95% confidence level. Feed (f) and depth of cut (a_p) were always kept as 0.1 mm and 0.5 mm respectively in every test, levels there are considerably low because they are parameters for finishing operations. Every experiment was performed twice.

3 Results and discussion

Figure 3 shows the results of cutting power consumption for all experiments at both the beginning (Fig. 3a) and the end of tool life (Fig. 3b). At the end of tool life when the cutting power was measured, the different experiments had different

cutting times. However, at this moment, flank wear was about the same for all experiments, i.e., $V_B = 0.3$ mm. Horizontal bars present the average volume between replicas and the error bar the standard deviation. It can be clearly seen that tool wear increased cutting power (compare Fig. 3a with Fig. 3b) considering a 95% confidence level, as it could be expected, as the growth of flank wear enlarges the contact area between tool and workpiece, increasing friction and consequently the main cutting force and cutting power. It can be also verified that this difference was more remarkable when high-pressure coolant was applied. Moreover, this cooling condition provided lower cutting power in comparison to conventional cooling, what can be associated either to the improvement of lubrication on the tool-chip interface, (a less probable hypothesis because due to the seizure zone which occurs between chip and tool rake face when machining ductile materials), or

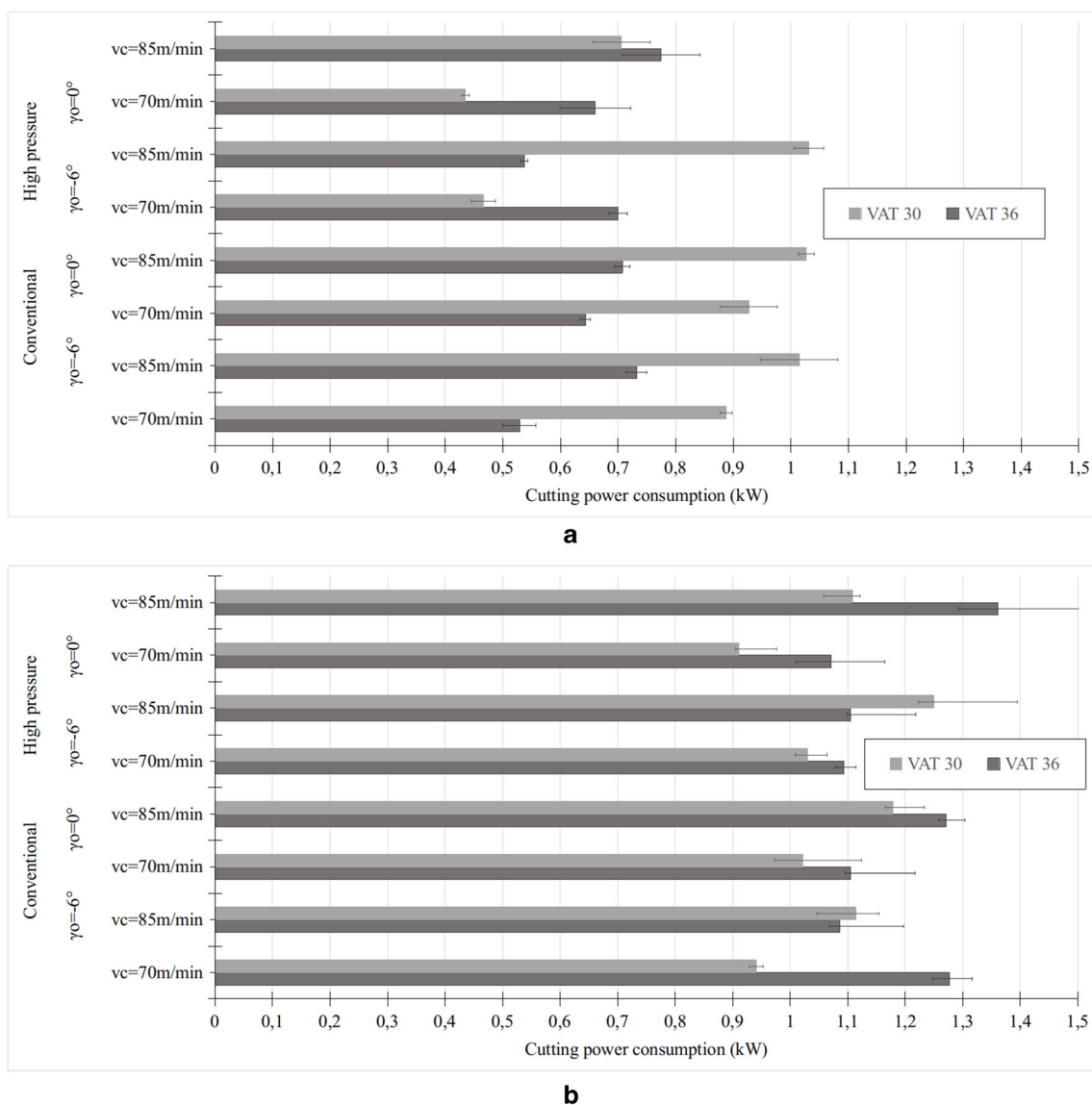


Fig. 3 Cutting power consumption at **a** the beginning of tool life and **b** the end of tool life

to the reduction of the contact area between tool and chip provided by the wedge effect of the high-pressure coolant. This fact has been observed in half of the experiments with VAT 30® and in almost every experiment regarding VAT 36®, except for negative tool and 85 m/min.

It is interesting to highlight that the use of a neutral tool provided lower cutting power consumption (as it was previously expected) than the negative rake angle tool only at the condition in which cutting speed had been set to 85 m/min and high-pressure coolant was used. At the other conditions, that is, with conventional cooling and/or lower cutting speed, this variation was not noticed, which means that the influence of the cooling condition and cutting speed may affect cutting power heavier than cutting tool geometry.

Finally, regarding the comparison between VAT 30® and VAT 36®, it can be seen that cutting power consumption was higher when machining VAT 36® in only three conditions, while it was higher for the cutting of VAT 30® in other five conditions. It is important to observe that, in one of the conditions in which power consumption was higher for VAT 36®, the measured difference has been barely remarkable. Then, it can be said, in a general way, that turning VAT 30® may require higher cutting power than VAT 36®, what is absolutely expected as the former presents higher hardness and ultimate tensile strength (see Table 3), which means higher energy demanded to shear the chips. Besides that, VAT 30® exhibits a larger strain hardening exponent, and so for successive passes (in the turning experiments, the tool successively passed on the workpiece decreasing its diameter in each pass), the tool was facing harder surfaces. It is important to remember that, due to the heat treatment made on the workpiece, there was a variation of hardness along the workpiece radius. However, since the depth of cut used was small (0.5 mm), it can be considered that this variation from one tool pass to the next was negligible and the hardness workpiece difference from one pass to the other is just caused by the strain hardening.

It is necessary to justify why cutting power consumption was lower for the cutting of VAT 30® than for VAT 36® in the turning experiment using high-pressure coolant, 70 m/min cutting speed for both tool geometries. The hypothesis is that lower cutting speed has made it possible for the high-pressure coolant to reach the zone between the rake face of the tool and the chip. As VAT 30® presents smaller elongation than VAT 36®, the chip has not spread out too much on the rake face of the tool, which makes lubrication easier. Then, in these conditions, more efficient lubrication has overcome the influence of the mechanical properties in such a way that power consumption was lower for VAT 30®.

Figure 4 shows the results for arithmetical mean roughness value (R_a) of the machined surface in each experiment measured at both the beginning (Fig. 4a) and the end of tool life (Fig. 4b). Horizontal bars present the average volume between

replicas and the error bar the standard deviation. In terms of cooling condition, in general, when high-pressure cooling was used, workpiece roughness was lower than when conventional cooling was used, very likely due to the higher lubrication provided by the former. This has been observed in any condition in the turning of VAT36® and almost in any condition for the VAT30® turning, except for the neutral tool and 85 m/min. In terms of cutting speed influence, nothing can be said considering a 95% confidence level, since for some experiments using $v_c = 70$ m/min, roughness was lower, and for other experiments, roughness was lower when 85 m/min was used. The same can be said in terms of tool geometry. This parameter also did not influence surface roughness in a consistent way. Comparing Fig. 4a with b, the influence of tool wear can be evaluated. Also in this comparison, there is no consistent tendency, since, for some experiments, roughness was higher when tool wear was high and, for others, roughness values were similar at the end and at the beginning of tool life. This result shows that the flank wear (which was the wear parameter used to define tool life) was probably not accompanied by the variation of the tool nose shape, which would cause the increase of roughness.

Comparing the turning operation on VAT 30® and VAT 36® in terms of surface roughness, only in two tests VAT 30® workpieces have presented rougher surfaces; actually, in only one roughness was reasonably higher. In three conditions, surface roughness was quite similar for the two valve steel alloys. In the other three tests, VAT 30® workpieces have presented considerably lower roughness than VAT 36®. On the other hand, it is difficult to correlate this result with the levels of the other variables, that is, cooling condition, tool geometry, and cutting speed. In other words, the conditions in which VAT30® surface roughness was lower than VAT36® roughness did not follow any pattern. Anyway, it can be said generally that VAT 30® produced lower or equal surface roughness than that VAT 36® considering a 95% confidence level. The reason for that is the lower ductility of VAT30®, which may be inferred by its lower elongation (Table 3). This feature made the plastic deformation of the VAT30® machined surface to be lower. The deformation of the surface becomes roughness; in other words, when a thin layer on the workpiece surface is plastically deformed, it does not return to its initial microscopic form, i.e., small variations of the flat form can be measured, which means surface roughness variation.

Nonetheless, there are other two factors that severely impair surface roughness: kinematics and dynamics. Tool radius and feed rate (both are fixed in this work) provide what is called kinematic roughness, that is, the arc shape on the machined surface that is inherent to the turning operation. Regarding dynamics, both tool and/or workpiece may vibrate during machining; but, in this case, they are considerably stiff, so that vibration has probably not influenced the results. In this case, the influence of the feature plasticity/ductility was

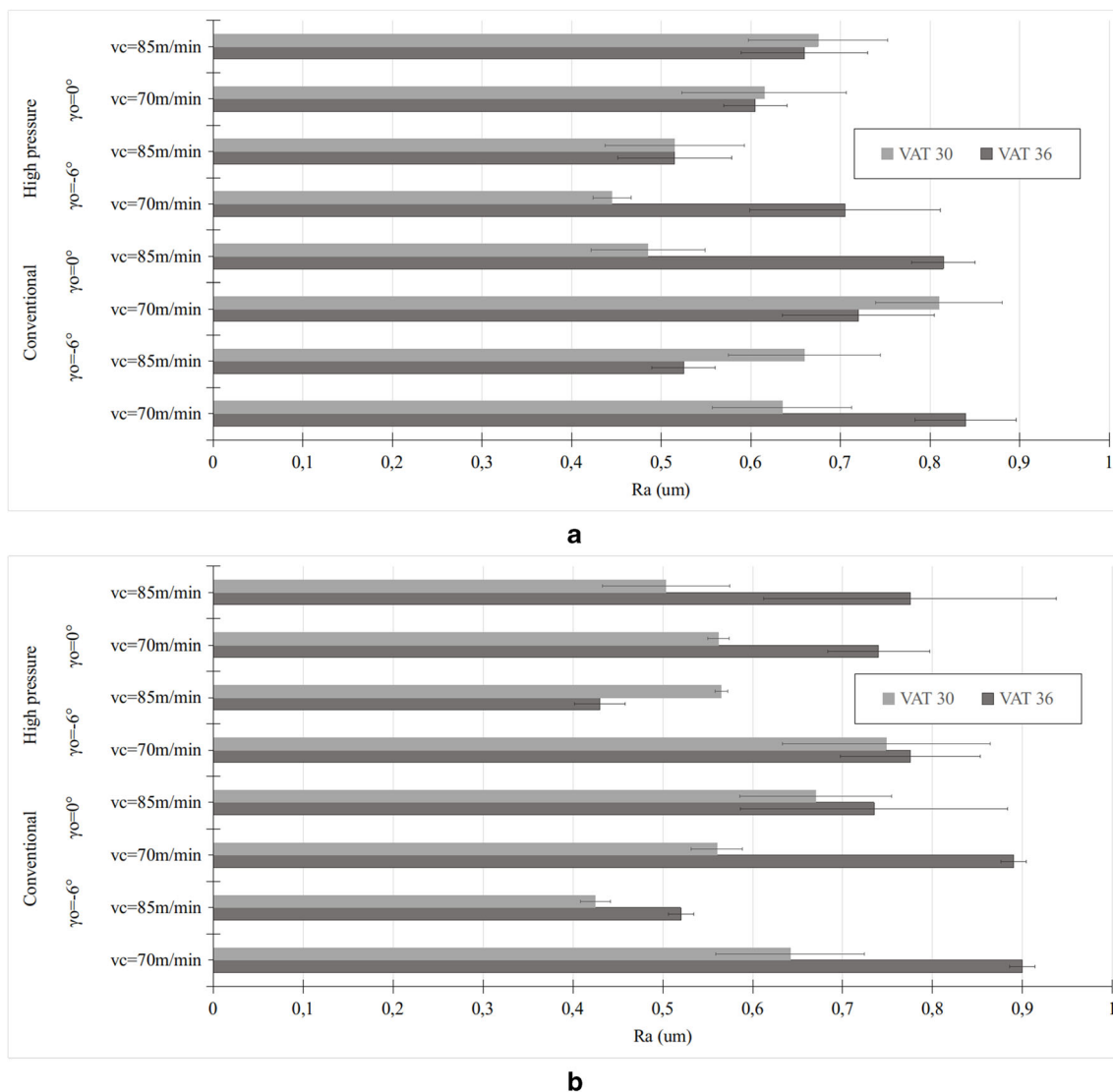


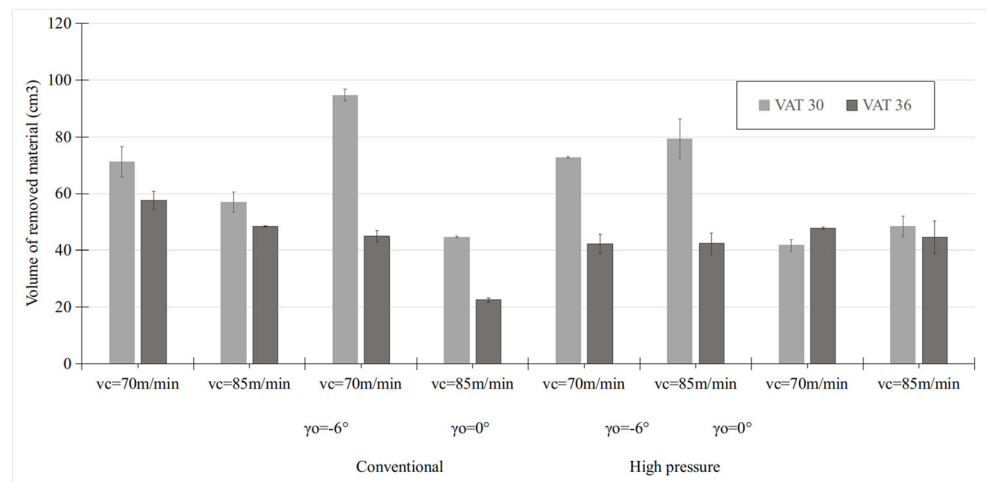
Fig. 4 Arithmetic mean roughness at **a** the beginning of tool life and **b** the end of tool life

predominant and made the VAT30® roughness to be, generally, lower than the VAT36® roughness.

Figure 5 shows results for the volume of material removed per tool life (V , cm^3) as calculated by Eq. 1 regarding each experiment. The vertical bars present the average volume between replicas and the error bar the standard deviation. It is expected that a higher cutting speed would severely impair tool life, as this influence is extensively reported in the literature [18]. The increase of cutting speed provides higher generation of heat in the process but the area of the tool which is exposed to this heat is the same, so that the temperature on the tool increases and then tool life decreases. It can be seen in the figure that for all tests using conventional cooling, as the cutting speed increased, tool life decreased. However, when high-pressure coolant was applied, this influence cannot be seen. Therefore, the improvement of cooling lubrication could even overcome the negative effect of the increase of cutting speed on tool life.

In general, the neutral tool has obtained shorter tool lives than the negative rake angle tool. Although negative tools provide more strained chips and larger friction contact area between tool and chip and, consequently, more heat generation, it presents bigger wedge angle, and then more volume to distribute the thermal input during the cut, so that the temperature on the tool is lower than what is verified when the neutral tool was applied. Moreover, due to the higher wedge angle, the same value of flank wear (V_{BBmax}) removes a larger amount of tool material when negative rake angle is used.

High-pressure coolant did not provide the longer tool life that was expected when compared to conventional cooling. In most experiments, when these two conditions were compared, sometimes high pressure presented longer lives, sometimes conventional cooling presented longer lives. Actually, only in the experiment with neutral tool and cutting speed of 70 m/min the life of the tool which cut VAT30® was considerably longer (more than two times longer) when conventional

Fig. 5 Tool life for all tested conditions

cooling was used. This is an indication that, due to the seizure conditions on the tool-chip interface, the high pressure of the fluid could not efficiently cool down the cutting edge.

It can be easily noticed that VAT 30® provided better results than VAT 36® in terms of tool life at almost every tested condition considering a 95% confidence level. Only for high-pressure coolant with neutral tooling ($\gamma_0 = 0^\circ$) and lower cutting speed 70 m/min the opposite is verified. Comparing the physical and mechanical properties of these two superalloys (Tables 2 and 3), part of them is favorable to the lower machinability of VAT 30®, part of them is favorable to the lower machinability of VAT 36®. The first one presents higher hardness, higher ultimate tensile strength, higher strain hardening exponent, and lower thermal conductivity features that would indicate it as the candidate to have the lowest machinability, which did not happen. According to Stahl et al. [7], each percent added in ultimate tensile stress promotes an increase of 1% in cutting temperature; on the other hand, an increase of 1% of the thermal conductivity decreases 10 °C in cutting temperature, as a higher amount of the heat generated in machining may be carried by chip or even workpiece. Similarly, a higher strain hardening exponent might decrease tool life. On the other hand, abrasiveness, elongation, and specific heat also impair tool life negatively; and VAT 30® exhibits lower values than VAT 36® for these three features (the difference of specific heat between the two alloys is less than 2%). The decrease of 1% of the specific heat means the reduction of several degrees Celsius in cutting temperature. Shorter elongation provides lower spreading out of the chip on the tool rake face, avoiding excessive warming of the tool and minimizing the attrition wear mechanism. Lower abrasiveness reduces the development of abrasion wear mechanism obviously.

Therefore, it is necessary to analyze the tool wear mechanism to verify which material property was predominant to make the tool to reach its end of life and, consequently, to understand why a material with higher hardness, higher

ultimate tensile strength, higher strain hardening exponent, and lower thermal conductivity like VAT30® presented longer tool life than VAT36®. Figure 6 provides a sample of the phenomena that have led to the end of tool life on both turning of VAT 30® (Fig. 6a) and VAT 36® (Fig. 6b). The pictures of this figure were taken on SEM after tests in which conventional cooling, neutral tool, and 70 m/min cutting speed were employed. The images of the tools used in the other experiments will not be shown because all of them have seemed quite similar to each other.

EDS analysis has shown elements from tool coating, that is, Ti, Al, and Cr (points 1 and 2 both in Fig. 6a and b), from substrate, that is W and Co (point 5 in Fig. 6a and points 7, 8, and 9 in Fig. 6b), and from workpiece material adhered, that is Fe, Ni, and Cr (points 3 and 4 in Fig. 6a and points 3, 4, 5, and 6 in Fig. 6b), either for VAT 30® or VAT 36® turning. Besides that, the presence of parallel abrasive scratches in the flank face of those tools is also indicated. Then, it is quite possible that abrasion wear was the main mechanism that has led to the removal of the tool coating, which, when present, could avoid, or at least make difficult, the adhesion of the material of the workpieces. After the removal of the coating, part of the material of the chip being formed was extruded between tool and workpiece and adhered to the flank face of the tool. This adhered material was capable of reaping out both tool substrate material and even more coating material by what is called attrition mechanism. Although cooling condition, tool geometry of cutting speed could accelerate or slow down tool wear, the same tool wear mechanisms were found in every experiment.

As attrition and abrasion were the main tool wear mechanisms found on turning of VAT 30® and VAT 36® in every tested condition, it is not difficult to say that the lower abrasiveness and elongation of the first superalloy could protect the tool against rapid wear caused by attrition (due to its lower elongation/ductility) and abrasion (due to its lower abrasiveness), in order to make tool life longer in almost every

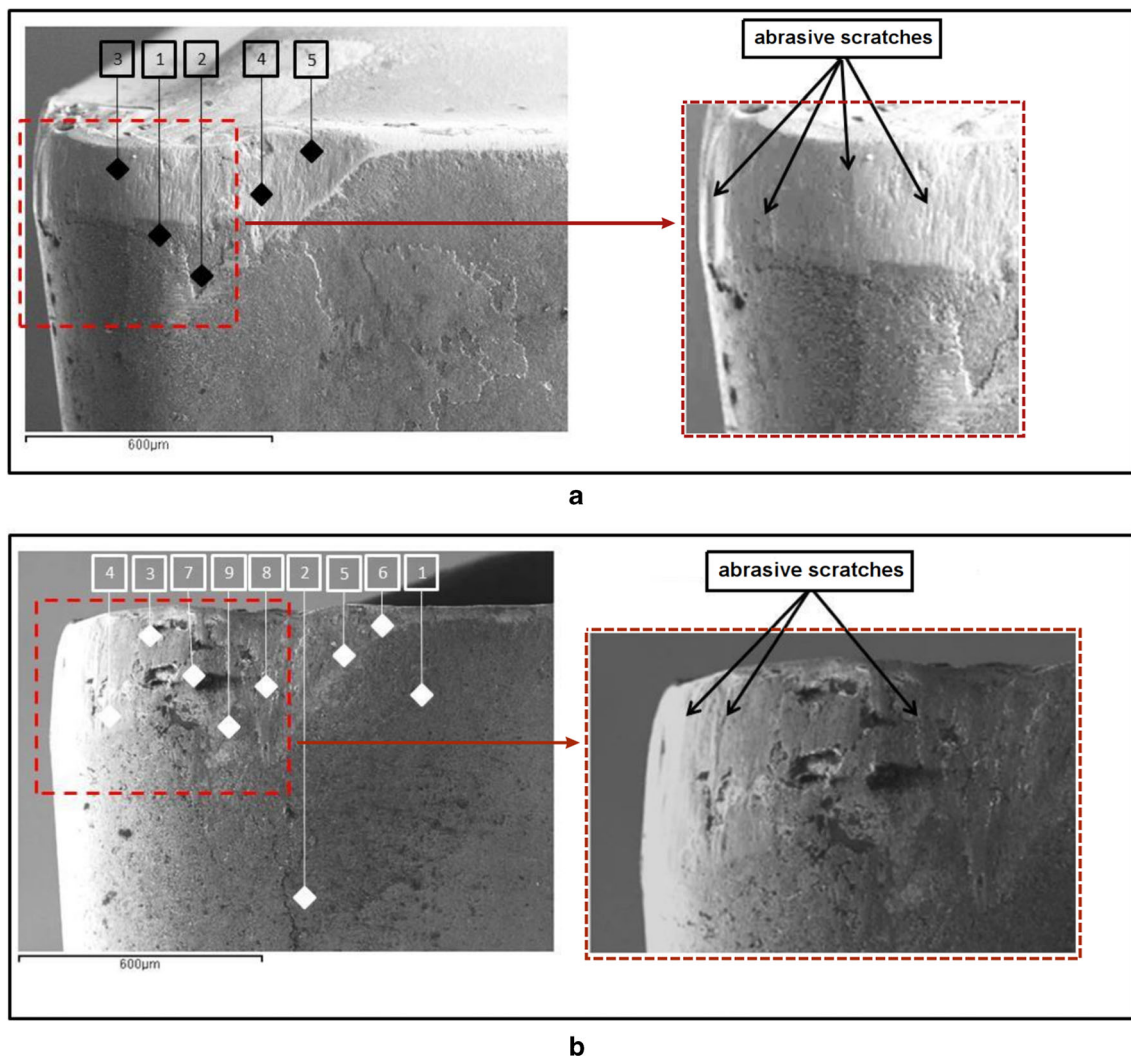


Fig. 6 SEM images at the end of tool life with conventional cooling, neutral tool, and 70 m/min cutting speed on **a** VAT 30@ and **b** VAT 36@ turning

experiment with VAT 30@ in comparison to VAT 36@. Therefore, the machinability of a material cannot be established based just on properties like hardness, tensile stress, strain hardening ratio, and thermal conductivity (remember that VAT 30@ has higher hardness, tensile stress, and strain hardening ratio than VAT36@ and lower thermal conductivity than VAT36@). Other properties like ductility/elongation and abrasiveness must be considered to establish its machinability, since they are very important in the definition of the tool wear mechanism.

4 Conclusions

Comparing the machinability of VAT 30@ and VAT 36@ iron-based superalloys, regarding finish turning, it can be generally said that tool life was longer when machining the first one than when machining the last one. This was not expected, since VAT 30@ presents higher hardness, ultimate tensile

strength, and strain hardening exponent, besides lower thermal conductivity.

The main tool wear mechanisms observed were abrasion and attrition, regardless of the valve steel that was being machined. As VAT 30@ also presents lower ductility and abrasiveness than VAT 36@, tool lives must have been longer for the first one because these properties retard both abrasion and attrition wear mechanisms.

Cutting power consumption is higher when machining VAT 30@ because of its higher mechanical strength, hardness, and strain hardening exponent.

Regarding surface roughness, VAT 30@ tends to provide equal or lower roughness than VAT 36@ due to the lower ductility of the former.

The machinability comparison in terms of tool life of two alloys must be done not just based on their macroscopic properties like hardness and tensile strength, but also on microscopic properties such as abrasiveness, since these properties also influence the tool wear mechanisms and, consequently, tool lives.

When the machinability comparison is made in terms of cutting power, the mechanical properties which must be taken into consideration are mechanical strength, hardness, and strain hardening exponent.

When the machinability comparison is made in terms of surface roughness, the alloy ductility is the most important property to be taken into consideration.

Acknowledgments The authors acknowledge the Coordination of Superior Level Staff Improvement (Capes) for providing the scholarship, Villares Metals for providing the valve steels for the cutting tests, and Sandvik Coromant for providing the cutting tools.

References

- Pierce D et al (2019) High temperature materials for heavy duty diesel engines: historical and future trends. *Prog Mater Sci*. <https://doi.org/10.1016/j.pmatsci.2018.10.004>
- Farina AB, Liberto RCN, Barbosa CA (2013) Desenvolvimento de novos aços válvula para aplicação em motores de alto desempenho. *Tecnol Metal Mater Min*. <https://doi.org/10.4322/tmm.2013.043>
- Silva ALVC, Mei PR (2006) *Aços e Ligas Especiais*. Blucher, São Paulo
- Ezugwu EO (2005) Key improvements in the machining of difficult-to-cut aerospace superalloys. *Int J Mach Tool Manu*. <https://doi.org/10.1016/j.ijmachtools.2005.02.003>
- Zimmerman C, Boppana SP, Katbi K (1990) Machinability test. In: *Metals handbook*, v. 16, 10th edn. ASM International, Metals Park, pp 639–647
- Yamane Y, Sekyia K, Narutaki N, Ezugwu EO (2006) Difficulty in machining calculated from mechanical and thermal properties of difficult to cut material. *Int C Prog Mach Technol* 8:497–501
- Stahl JE et al (2012) Metal cutting theories and models. Lund University Press. In: Lund
- Asha PB et al (2018) Effect of machining parameters on cutting tool temperature and tool life while turning EN24 and HCHCr grade alloy steel. *Mater Today-Proc*. <https://doi.org/10.1016/j.matpr.2018.02.152>
- Vinoth Jebaraj A et al (2017) Weldability, machinability and surfacing of commercial duplex stainless steel AISI2205 for marine applications - A recent review. *J Adv Res*. <https://doi.org/10.1016/j.jare.2017.01.002>
- Denkena B et al (2015) Effects of alloying elements in UHC-steels and consequences for the machinability. *CIRP J Manuf Sci Technol*. <https://doi.org/10.1016/j.cirpj.2015.04.001>
- Rocha CA et al (2004) Evaluation of the wear mechanisms and surface parameters when machining internal combustion engine valve seats using PCBN tools. *J Mater Process Technol*. <https://doi.org/10.1016/j.jmatprotec.2003.10.004>
- Liu G et al (2017) The modified surface properties and fatigue life of Incoloy A286 face-milled at different cutting parameters. *Mat Sci Eng Struct*. <https://doi.org/10.1016/j.msea.2017.07.072>
- Tian X et al (2018) Performance of Si₃N₄/(W, Ti)C graded ceramic tool in high-speed turning iron-based superalloys. *Ceram Int*. <https://doi.org/10.1016/j.ceramint.2018.05.222>
- Davoodi B, Eskandari B (2015) Tool wear mechanisms and multi-response optimization of tool life and volume of material removed in turning of N-155 iron–nickel-base superalloy using RSM. *Measurement*. <https://doi.org/10.1016/j.measurement.2015.03.006>
- Ferraresi D (1970) *Usinagem dos metais*. Blucher, São Paulo
- Buttery TC, Archard JF (1971) Some microscopical investigations of grinding and abrasive wear. *J Microsc-Oxford*. <https://doi.org/10.1111/j.1365-2818.1971.tb02357.x>
- Diniz AE et al (2014) *Tecnologia da Usinagem dos Materiais*. Artliber, São Paulo
- Trent EM, Wright PK (2000) *Metal cutting*. Butterworth-Heinemann, Woburn
- Villares Metals (2013) *Ligas intermediárias de Níquel*. Villares Metals S.A. <http://www.villaresmetals.com.br/villares/pt/Produtos/Acos-Valvula>. Accessed 05 March 2019

Publisher's note Springer Nature remains neutral with regard to jurisdictional claims in published maps and institutional affiliations.